

Quasielastic electron scattering on a two-nucleon model system: Scaling and cumulant expansion of the structure function

D. Hüber, W. Glöckle, and A. Bömelburg

Institut für Theoretische Physik II, Ruhr-Universität Bochum, D-4630 Bochum 1, Federal Republic of Germany

(Received 12 February 1990)

The structure function $S(q, \omega)$ for quasielastic electron scattering on a nonrelativistic two-nucleon model system is evaluated numerically. These S values are considered as pseudodata to study sum rules, y scaling, and the cumulant expansion. For the force models considered it is found that the reduced structure function $(q/2m)S(q, \omega)$ in the limit $q \rightarrow \infty$ scales to the longitudinal momentum distribution $P_L(y)$ in the target. Except for small y values, this limit, however, is reached only very slowly, which may be due to the strictly nonrelativistic treatment. The cumulant expansion based on low-order cumulants is not useful. We also derive the analytical result that in our potential model $S(q, \omega) = O(\omega^{-5.5})$ for $\omega \rightarrow \infty$ and fixed q . This shows that higher-order cumulants do not exist.

I. INTRODUCTION

Inclusive electron scattering on a nuclear target provides through the structure function an important insight into the dynamics of the target constituents. The structure function S depends on the energy ω and the magnitude of the three-momentum q transferred to the target. What are the properties of that function, especially for large values of q and ω ? We investigate this question in the context of a nonrelativistic potential model of two "nucleons," which interact by a potential with range and strength typical for the NN force. Our study is stimulated by the classical review on electron scattering.¹ There it is shown that $(q^2/4m)S(q, \omega) \rightarrow \delta(\eta - 1)$ for $q \rightarrow \infty$ with $\eta = \omega/(q^2/2m)$. This simply reflects the quasielastic scattering on a constituent with mass m . According to the notation chosen in Ref. 1 it may be called ξ scaling ($\xi \equiv 1/\eta$), a scaling behavior which can be regarded as a nonrelativistic analogue to the relativistic Bjorken scaling. What is the leading correction term, which breaks that scaling behavior? What is its power law in q and which dynamical information can be inferred from it? We shall show that it is again a distribution. A possibly useful and immediate consequence are sum rules. Of course they can also be established by standard steps, which, however, hide their connection to ξ scaling and to the term breaking ξ scaling in leading order. In Ref. 1 it is also shown that $(q/2m)S(q, \omega) \rightarrow P_L(y)$ for $q \rightarrow \infty$ with $y = (q/2)(\eta - 1)$. Here $P_L(y)$ is the distribution of momentum components $p_{\parallel} \equiv \mathbf{p} \cdot \hat{\mathbf{q}}$ in the target. This would be a very desirable information about the target if it could be extracted from the structure function in a model-independent way. At which q 's is this reliably possible, if at all? How important is the final-state interaction in the evaluation of the structure function?

In Ref. 2 the structure function is examined in terms of a few cumulants which serve to characterize the position, height, and width of the quasielastic peak. Is the cumulant expansion quantitatively useful in the sense that a fit of that form to a given (experimental) structure function

leads to reliable values of the cumulants? This would be useful since the low-order cumulants have a physical meaning. In this context we pose the question of whether cumulants of higher orders exist at all. This depends on the asymptotic behavior of $S(q, \omega)$ for $\omega \rightarrow \infty$ and q fixed. Does it decrease exponentially or only like an inverse power law?

We study these questions in a strictly nonrelativistic context. We are aware of the physical limitations of that model, especially in view of the high momentum transfers which we will see to be necessary to reach really the domain of scaling. Insofar as this study is academic, however, the insight we shall gain may be valid qualitatively also in a future study including relativity (not only relativistic kinematics). Similar studies in potential models have been carried through.^{2,3} Here quasielastic scattering on one particle bound in a square well or Woods-Saxon potential has been investigated numerically. We perform a study on two strongly interacting particles which are either both charged, allowing us to see interference effects, or where only one particle is charged. The latter case corresponds to the previous studies^{2,3} of one particle bound in a potential. The final-state interaction of the two outgoing "nucleons" turns out to be very crucial. Since their energy of relative motion can be very high, a partial-wave expansion is not very adequate and may be very unreliable. In Ref. 3 numerical difficulties were pointed out in that context. We allow the two "nucleons" to interact in all partial waves and keep the scattering angle as a dynamical variable instead of using orbital angular momenta. This is a much better representation of the two-body T matrix which is considerably peaked in forward directions than building up T by strongly oscillating partial-wave contributions. In addition our interaction, superposition of Yukawas in the form of the Malfliet-Tjon potential (MT III) (Ref. 4) are "closer" to the reality of NN forces than a square well potential. We assume the potential to be local and therefore to act in all partial waves (not only in s states). In this model we are able to provide analytical insight and to

solve the numerical part exactly, since we work with three-vectors.

In Sec. II we define the model and formulate the exact expression for the structure function suitable for the numerical evaluation. The ξ scaling and the leading correction term are derived in Sec. III. There we also set up the sum rules. In Sec. IV we review the y scaling and in Sec. V the cumulant expansion of S . In Sec. V we also derive the asymptotic ω dependence of S for fixed q . Section VI describes our numerical techniques and there we show and discuss the numerical results. Finally, we present a summary in Sec. VII.

II. THE MODEL AND ITS STRUCTURE FUNCTION

We regard two spinless "nucleons" which are both equally charged and interact by a local potential, which supports one bound state with a binding energy of $e = -2.23$ MeV. Charging both nucleons leads to coherent and incoherent contributions to the structure function and we shall get a rough idea of what will happen in ${}^3\text{He}$. We also regard the case of a model deuteron, where only one "nucleon" is charged. The longitudinal structure function for nonrelativistic nucleons is^{1,2}

$$S(q, \omega) \equiv \sum_f |\langle \varphi_f | e^{(i/2)q \cdot r} + e^{-(i/2)q \cdot r} | \varphi \rangle|^2 \times \delta \left[\omega + e - e_f - \frac{q^2}{4m} \right]. \quad (2.1)$$

Here the operator in the matrix element is

$$\rho(\mathbf{q}) = \sum_{i=1}^2 e^{i\mathbf{q} \cdot \mathbf{x}_i}, \quad (2.2)$$

the single-particle density for point nucleons in the c.m. system ($\mathbf{r} \equiv \mathbf{x}_1 - \mathbf{x}_2$) for a given three-momentum transfer to the target, φ is the two-body bound state, and the sum over f includes φ and the two-body scattering states $\varphi_{\mathbf{p}}^{(+)}$ in the potential V . The argument of the δ function describes energy conservation in the laboratory system: the transferred energy ω together with the binding energy $e < 0$ is equal to the c.m. energy of the two nucleons $q^2/4m$ and the internal energy e_f , which is either $e \equiv -\kappa^2/m$ (elastic scattering) or p^2/m (breakup process).

In explicit momentum-space representation, Eq. (2.1) reads

$$S = 4 \left| \int d\mathbf{p} \varphi \left[\mathbf{p} + \frac{\mathbf{q}}{2} \right] \varphi(p) \right|^2 \delta \left[\omega - \frac{q^2}{4m} \right] + \int d\mathbf{p} \left| \int d\mathbf{p}' \varphi_{\mathbf{p}'}^{(+)*}(\mathbf{p}') \left[\varphi \left[\mathbf{p}' - \frac{\mathbf{q}}{2} \right] + \varphi \left[\mathbf{p}' + \frac{\mathbf{q}}{2} \right] \right] \right|^2 \delta \left[\omega + e - \frac{p^2}{m} - \frac{q^2}{4m} \right]. \quad (2.3)$$

The factor of 4 results from the permutation symmetry of φ . The momentum space representation of the two-body scattering state is

$$\varphi_{\mathbf{p}}^{(+)}(\mathbf{p}') = \delta(\mathbf{p} - \mathbf{p}') + \frac{T(\mathbf{p}', \mathbf{p})}{(p^2/m) + i\epsilon - (p'^2/m)}, \quad (2.4)$$

where T is the half-shell two-body T matrix and obeys the Lippmann-Schwinger equation

$$T(\mathbf{p}', \mathbf{p}) = V(\mathbf{p}', \mathbf{p}) + \int d\mathbf{p}'' V(\mathbf{p}, \mathbf{p}'') \frac{1}{(p^2/m) + i\epsilon - (p''^2/m)} T(\mathbf{p}'', \mathbf{p}). \quad (2.5)$$

Since we are interested only in inelastic scattering we regard only the second part in Eq. (2.3) which inserting Eq. (2.4) is

$$S_C = \int d\mathbf{p} \left| \varphi \left[\mathbf{p} - \frac{\mathbf{q}}{2} \right] + \varphi \left[\mathbf{p} + \frac{\mathbf{q}}{2} \right] + \int d\mathbf{p}' \frac{T^*(\mathbf{p}', \mathbf{p})}{(p^2/m) - i\epsilon - (p'^2/m)} \left[\varphi \left[\mathbf{p}' - \frac{\mathbf{q}}{2} \right] + \varphi \left[\mathbf{p}' + \frac{\mathbf{q}}{2} \right] \right] \right|^2 \delta \left[\omega + e - \frac{p^2}{m} - \frac{q^2}{4m} \right]. \quad (2.6)$$

The first part alone stems from the free two-nucleon states and the second part proportional to T^* incorporates the final-state interaction of the two outgoing nucleons. In our model the two-body bound state is a pure s state. The scalar potential V leads to a scalar T matrix:

$$T(\mathbf{p}', \mathbf{p}) = T(p', p, \hat{\mathbf{p}}' \cdot \hat{\mathbf{p}}). \quad (2.7)$$

We end up with

$$S_C = \pi m k \int_{-1}^{+1} dt \left| \varphi \left[\left(k^2 + \frac{q^2}{4} - kqt \right)^{1/2} \right] + \varphi \left[\left(k^2 + \frac{q^2}{4} + kqt \right)^{1/2} \right] \right. \\ \left. + \int_0^\infty dp' \frac{p'^2}{(k^2/m) - i\epsilon - (p'^2/m)} \int_{-1}^{+1} dt' \left[\varphi \left[\left(p'^2 + \frac{q^2}{4} - p'qt' \right)^{1/2} \right] + \varphi \left[\left(p'^2 + \frac{q^2}{4} + p'qt' \right)^{1/2} \right] \right] \right. \\ \left. \times \int_0^{2\pi} d\phi' T^*(p', k, \cos\theta) \right|^2, \quad (2.8)$$

where

$$\cos\theta = tt' + (1-t^2)^{1/2}(1-t'^2)^{1/2}\cos\phi' \quad (2.9)$$

and

$$k = \left[m(\omega + e) - \frac{q^2}{4} \right]^{1/2}. \quad (2.10)$$

We choose two types of “two-nucleon interactions:”

$$V(r) = V_1 \frac{e^{-\mu_1 r}}{r} + V_2 \frac{e^{-\mu_2 r}}{r} \quad (2.11)$$

and

$$V(r) = V_0 e^{-\mu r}. \quad (2.12)$$

They are supposed to be local and act in *all* partial waves. The expression (2.8) will be evaluated numerically and delivers pseudodata for the structure function, which will be analyzed with respect to scaling behavior, sum rules, and the cumulant expansion.

In the case that only one nucleon is charged, there is only one term in (2.2) and so the two sums over two bound-state wave functions are replaced by just one term, respectively.

The asymptotic behavior of the two-body bound-state wave function $\varphi(p)$ for $p \rightarrow \infty$ will be important in the following. It is connected to the configuration space wave function by

$$\varphi(p) = \frac{4\pi}{(2\pi)^{3/2}} \int_0^\infty dr r^2 j_0(pr) \varphi(r). \quad (2.13)$$

Simple partial integrations yield, for $p \rightarrow \infty$,

$$S = \sum_f \langle \varphi | (e^{(i/2)q \cdot r} + e^{-(i/2)q \cdot r}) \delta \left[\omega + e - H - \frac{q^2}{4m} \right] | \varphi_f \rangle \langle \varphi_f | e^{(i/2)q \cdot r} + e^{-(i/2)q \cdot r} | \varphi \rangle \\ = \langle \varphi | (e^{(i/2)q \cdot r} + e^{-(i/2)q \cdot r}) \delta \left[\omega + e - H - \frac{q^2}{4m} \right] (e^{(i/2)q \cdot r} + e^{-(i/2)q \cdot r}) | \varphi \rangle. \quad (3.3)$$

We introduced the two-body Hamiltonian

$$H = H_0 + V \quad (3.4)$$

with the eigenfunctions φ and φ_f . Expression (3.3) can be rewritten as³

$$S = -\frac{1}{\pi} \text{Im} \langle \varphi | (e^{(i/2)q \cdot r} + e^{-(i/2)q \cdot r}) \frac{1}{\omega + e - H - (q^2/4m) + i\epsilon} (e^{(i/2)q \cdot r} + e^{-(i/2)q \cdot r}) | \varphi \rangle. \quad (3.5)$$

$$\varphi(p) \xrightarrow{p \rightarrow \infty} -\frac{8\pi}{(2\pi)^{3/2}} \frac{\varphi'(r=0)}{p^4} \equiv \frac{C}{p^4}. \quad (2.14)$$

In the case of the Yukawa potentials [Eq. (2.11)] $\varphi'(r=0)$ is different from zero and is given by

$$\varphi'(r=0) = \varphi(r=0) \frac{m}{2} (V_1 + V_2). \quad (2.15)$$

Since we shall determine $\varphi(p)$ directly in momentum space (see Sec. VI), we use, in accordance with (2.13),

$$\varphi(r=0) = \frac{4\pi}{(2\pi)^{3/2}} \int_0^\infty dp p^2 \varphi(p). \quad (2.16)$$

In the case of the potential (2.12), one finds $\varphi'(r=0) = 0$ and the decrease is $O(1/p^6)$.

III. ξ SCALING

Let us first regard the case of the two charged “nucleons.” The dominance of quasielastic scattering at the constituents of the target should get more and more pronounced with increasing momentum and energy transfer. Indeed as shown in Ref. 1,

$$\frac{q^2}{4m} S \xrightarrow{q \rightarrow \infty} \delta(\eta - 1) \quad (3.1)$$

with

$$\eta \equiv 2m\omega/q^2 = \frac{1}{\xi}. \quad (3.2)$$

The case $\eta = \xi = 1$ describes the simple kinematic situation that all the energy ω is transferred into kinetic energy of one knocked out constituent. Here we are interested in looking for the leading correction term which breaks that scaling law. To this result we rewrite (2.1) as

For a local potential the Galilean transformation $e^{(i/2)q \cdot r}$ yields

$$e^{-(i/2)q \cdot r} H e^{(i/2)q \cdot r} = \frac{[\mathbf{p} + (\mathbf{q}/2)]^2}{m} + V. \quad (3.6)$$

Consequently,

$$\begin{aligned} S &= -\frac{2}{\pi} \text{Im} \langle \varphi | (1 + e^{iq \cdot r}) \frac{1}{\omega + e - \left[\left[\mathbf{p} + \frac{\mathbf{q}}{2} \right]^2 / m \right] - V - (q^2/4m) + i\epsilon} | \varphi \rangle \\ &= -\frac{1}{\pi} \frac{4m}{q^2} \text{Im} \langle \varphi | (1 + e^{iq \cdot r}) \frac{1}{\eta - 1 - (2p_{\parallel}/q) - (2m/q^2)(H - e) + i\epsilon} | \varphi \rangle \end{aligned} \quad (3.7)$$

with

$$p_{\parallel} \equiv \mathbf{p} \cdot \hat{\mathbf{q}}. \quad (3.8)$$

In the case of the one charged particle the factor of 4 is replaced by 2 and the interference term $e^{iq \cdot r}$ arising from the scattering at different particles is absent.

The typical finite momenta in the matrix element are determined by the bound-state wave function and the two-body force V . Hence, for q sufficiently large the denominator can be expanded:

$$\begin{aligned} \frac{q^2}{4m} S &= -\frac{1}{\pi} \text{Im} \langle \varphi | (1 + e^{iq \cdot r}) \left[\frac{1}{\eta - 1 + i\epsilon} + \frac{(2p_{\parallel}/q) + (2m/q^2)(H - e)}{(\eta - 1 + i\epsilon)^2} + \frac{[(2p_{\parallel}/q) + (2m/q^2)(H - e)]^2}{(\eta - 1 + i\epsilon)^3} + \dots \right] | \varphi \rangle \\ &= -\frac{1}{\pi} \text{Im} \langle \varphi | (1 + e^{iq \cdot r}) \left[\frac{1}{\eta - 1 + i\epsilon} + \frac{2p_{\parallel}/q}{(\eta - 1 + i\epsilon)^2} + \frac{(4p_{\parallel}^2/q^2) + (4m/q^3)[V, p_{\parallel}]}{(\eta - 1 + i\epsilon)^3} + \dots \right] | \varphi \rangle. \end{aligned} \quad (3.9)$$

In the last step we used $(H - e)\varphi = 0$.

With

$$\delta(\eta - 1) = -\frac{1}{\pi} \text{Im} \frac{1}{\eta - 1 + i\epsilon}, \quad (3.10)$$

and the derivatives thereof we get

$$\begin{aligned} \frac{q^2}{4m} S &= (1 + \langle \varphi | e^{iq \cdot r} | \varphi \rangle) \delta(\eta - 1) - \frac{2}{q} (\langle \varphi | p_{\parallel} | \varphi \rangle + \langle \varphi | e^{iq \cdot r} p_{\parallel} | \varphi \rangle) \delta'(\eta - 1) + (2/q^2) (\langle \varphi | p_{\parallel}^2 | \varphi \rangle + \langle \varphi | e^{iq \cdot r} p_{\parallel}^2 | \varphi \rangle) \delta''(\eta - 1) \\ &\quad + (2m/q^3) (\langle \varphi | [V, p_{\parallel}] | \varphi \rangle + \langle \varphi | e^{iq \cdot r} [V, p_{\parallel}] | \varphi \rangle) \delta''(\eta - 1) + \dots \end{aligned} \quad (3.11)$$

Note that all matrix elements are real and therefore the imaginary parts arise solely from the denominators. Obviously one has

$$\langle \varphi | p_{\parallel} | \varphi \rangle = 0, \quad (3.12)$$

$$\langle \varphi | [V, p_{\parallel}] | \varphi \rangle = 0, \quad (3.13)$$

and

$$\langle \varphi | p_{\parallel}^2 | \varphi \rangle = \frac{m}{3} \langle \varphi | H_0 | \varphi \rangle \equiv \frac{m}{3} \langle H_0 \rangle. \quad (3.14)$$

We thus obtain

$$\begin{aligned} \frac{q^2}{4m} S &= (1 + \langle \varphi | e^{iq \cdot r} | \varphi \rangle) \delta(\eta - 1) - \frac{2}{q} \langle \varphi | e^{iq \cdot r} p_{\parallel} | \varphi \rangle \delta'(\eta - 1) \\ &\quad + [(2m/3q^2) \langle H_0 \rangle + (2/q^2) \langle \varphi | e^{iq \cdot r} p_{\parallel}^2 | \varphi \rangle] \delta''(\eta - 1) + O(1/q^3). \end{aligned} \quad (3.15)$$

It is easily estimated using (2.14) that the interference terms behave asymptotically as⁵

$$\langle \varphi | e^{iq \cdot r} | \varphi \rangle = O \left[\frac{1}{q^4} \right], \quad (3.16)$$

$$\langle \varphi | e^{iq \cdot r} p_{\parallel} | \varphi \rangle = O \left[\frac{1}{q^3} \right], \quad (3.17)$$

$$\langle \varphi | e^{iq \cdot r} p_{\parallel}^2 | \varphi \rangle = O \left[\frac{1}{q^2} \right]. \quad (3.18)$$

Therefore we find in leading order in $1/q$,

$$\frac{q^2}{4m} S \rightarrow \delta(\eta - 1) + \frac{2m}{3q^2} \langle H_0 \rangle \delta''(\eta - 1), \quad (3.19)$$

which displays explicitly the ξ -scaling breaking term. In our model with $\langle H_0 \rangle = 10.8$ MeV

$$\frac{2m \langle H_0 \rangle}{3q^2} \approx \left[\frac{0.4 \text{ fm}^{-1}}{q} \right]^2. \quad (3.20)$$

In the case of the one charged particle the interference terms in Eq. (3.15) are absent and S is to be replaced by $2S$ in Eq. (3.19).

In order to extract the information $\langle H_0 \rangle$ from Eq. (3.19) it seems unavoidable to integrate the distributions with suitable functions, which naturally leads to sum rules. Possible functions are powers of $(\eta - 1)$ and we get three sum rules:

$$\frac{q^2}{4m} \int_{\eta_{\min}}^{\infty} d\eta S(q, \eta) \xrightarrow{q \rightarrow \infty} 1, \quad (3.21)$$

$$\frac{q^2}{4m} \int_{\eta_{\min}}^{\infty} d\eta (\eta - 1) S(q, \eta) \xrightarrow{q \rightarrow \infty} 0, \quad (3.22)$$

$$\frac{q^2}{4m} \int_{\eta_{\min}}^{\infty} d\eta (\eta - 1)^2 S(q, \eta) \xrightarrow{q \rightarrow \infty} (4m/3q^2) \langle H_0 \rangle. \quad (3.23)$$

Equation (3.21) is a normalization property. Integrating over ω instead of η the right-hand side will be 2, which measures the number of charged particles as is clear from the very definition [Eq. (3.1)] for S . The second sum rule tells that S is asymptotically an even function around $\eta = 1$. In the numerical evaluation in Sec. VI, we shall infer from these two sum rules the necessary range of η values and the q values beyond which the interference terms are negligible. The last sum rule is the interesting one since it delivers the expectation value of the kinetic energy in the ground state.

The lower limit of integration η_{\min} , referring to the continuum part S_C , follows from the energy conserving δ function in (2.1) and is

$$\eta_{\min} \equiv \frac{1}{2} - \frac{2me}{q^2}. \quad (3.24)$$

The elastic part of the structure function S_e , is proportional to $\delta(\eta - \frac{1}{2})$ as is obvious from Eq. (2.1) and does not contribute to Eqs. (3.21)–(3.23).

If one integrates (3.15) instead of (3.19) one arrives at the following three sum rules:

$$\frac{q^2}{4m} \int_{\eta_{\min}}^{\infty} d\eta S(q, \eta) = 1 + \langle \varphi | e^{iq \cdot r} | \varphi \rangle, \quad (3.25)$$

$$\frac{q^2}{4m} \int_{\eta_{\min}}^{\infty} d\eta (\eta - 1) S(q, \eta) = \frac{2}{q} \langle \varphi | e^{iq \cdot r} p_{\parallel} | \varphi \rangle, \quad (3.26)$$

$$\begin{aligned} \frac{q^2}{4m} \int_{\eta_{\min}}^{\infty} d\eta (\eta - 1)^2 S(q, \eta) \\ = \frac{4m}{3q^2} \langle H_0 \rangle + \frac{4}{q^2} \langle \varphi | e^{iq \cdot r} p_{\parallel}^2 | \varphi \rangle \\ + \frac{4m}{q^3} \langle \varphi | e^{iq \cdot r} [V, p_{\parallel}] | \varphi \rangle. \end{aligned} \quad (3.27)$$

In contrast to what one might expect these are exact relations except for corrections from the elastic channel which die out very quickly with increasing q . They also follow [Ref. 5] simply by standard steps from the very definition of S [Eq. (2.1)].

In the case of the one charged particle all the interference terms are absent and one arrives at Eqs. (3.21)–(3.23) valid now for *all* q , with S replaced by $2S$, again except for correction terms from the elastic channel. Particularly, the last sum rule may be of interest to extract $\langle H_0 \rangle$. We shall investigate this point for our pseudodata in Sec. VI.

IV. y SCALING

While $(q^2/4m)S$ tends towards a distribution for $q \rightarrow \infty$, the product $(q/2m)S$ tends towards a normal function and scales in the variable y :¹

$$y \equiv \frac{m}{q} \left[\omega - \frac{q^2}{2m} \right] = \frac{q}{2} (\eta - 1). \quad (4.1)$$

We introduce y in Eq. (2.7) and get

$$S = -\frac{1}{\pi} \frac{2m}{q} \text{Im} \langle \varphi | (1 + e^{iq \cdot r}) \frac{1}{y - p_{\parallel} - (\kappa^2 + p^2)/q - (mV/q) + i\epsilon} | \varphi \rangle. \quad (4.2)$$

Now one can expand⁶ for large q values:

$$\begin{aligned} \frac{q}{2m} S = -\frac{1}{\pi} \text{Im} \langle \varphi | (1 + e^{iq \cdot r}) \frac{1}{y - p_{\parallel} + i\epsilon} | \varphi \rangle - \frac{1}{\pi q} \text{Im} \langle \varphi | (1 + e^{iq \cdot r}) \frac{1}{y - p_{\parallel} + i\epsilon} (\kappa^2 + p^2 + mV) \frac{1}{y - p_{\parallel} + i\epsilon} | \varphi \rangle \\ + O \left[\frac{1}{q^2} \right]. \end{aligned} \quad (4.3)$$

The leading term is

$$-\frac{1}{\pi} \text{Im} \langle \varphi | \frac{1}{y - p_{\parallel} + i\epsilon} | \varphi \rangle = \int d\mathbf{p} |\varphi(p)|^2 \delta(y - p_{\parallel}) = \int d\mathbf{p}_{\perp} |\varphi((p_{\perp}^2 + y^2)^{1/2})|^2 \equiv P_L(y) \quad (4.4)$$

which apparently is the longitudinal momentum distribution in the state φ . For the numerical evaluation it is convenient to rewrite $P_L(y)$ as

$$P_L(y) = 2\pi \int_{|y|}^{\infty} dp p |\varphi(p)|^2. \quad (4.5)$$

As an example, we estimate the first interference term:

$$-\frac{1}{\pi} \text{Im} \langle \varphi | e^{iq \cdot r} \frac{1}{y - p_{\parallel} + i\epsilon} | \varphi \rangle = 2\pi \int_0^{\infty} dp_{\perp} p_{\perp} \varphi((y^2 + p_{\perp}^2)^{1/2}) \varphi([p_{\perp}^2 + (y+q)^2]^{1/2}). \quad (4.6)$$

For fixed y and $q \rightarrow \infty$ one can replace the second φ by its asymptotic form, Eq. (2.14), and find

$$2\pi C \int_0^{\infty} dp_{\perp} p_{\perp} \varphi((y^2 + p_{\perp}^2)^{1/2}) \frac{1}{(p_{\perp}^2 + q^2)^2} = O\left(\frac{1}{q^4}\right). \quad (4.7)$$

This term can therefore be safely neglected for large q values. The leading correction term to $P_L(y)$ is

$$-\frac{1}{\pi q} \text{Im} \langle \varphi | \frac{1}{y - p_{\parallel} + i\epsilon} (\kappa^2 + p^2 + mV) \frac{1}{y - p_{\parallel} + i\epsilon} | \varphi \rangle = \frac{1}{2q} \langle \varphi | \delta'(y - p_{\parallel}) (\kappa^2 + p^2) | \varphi \rangle - \frac{2m}{q} \langle \varphi | \delta(y - p_{\parallel}) V \frac{P}{y - p_{\parallel}} | \varphi \rangle, \quad (4.8)$$

where P denotes the principal value prescription. The matrix elements exist and are manifestly odd in y as is well known.⁶ The leading correction term is therefore only $O(1/q)$. This is also true in the case of the one charged particle. That contribution term vanishes in the quasielastic peak $y=0$. The related interference term is again of higher order in $1/q$.

V. CUMULANT EXPANSION AND ASYMPTOTIC BEHAVIOR OF $S(q, \omega)$ FOR $\omega \rightarrow \infty$

In Ref. 2 Rosenfelder advocated the use of a few low-order cumulants for the representation of the Fourier transform of S in order to parametrize location, width, and height of the quasielastic peak. We shall apply that concept to our model case. Let

$$S(q, \omega) \equiv \frac{m_0}{2\pi} \int_{-\infty}^{+\infty} dt e^{-i\omega t} F(t), \quad (5.1)$$

where

$$\omega' \equiv \omega - \frac{q^2}{4m} \quad (5.2)$$

is the energy transfer into internal motion. The moments of S are defined by

$$m_k \equiv \int_0^{\infty} d\omega' \omega'^k S(q, \omega), \quad (5.3)$$

which according to Eq. (3.3) can be written as

$$m_k = \langle \varphi | A^{\dagger} (H - e)^k A | \varphi \rangle \quad (5.4)$$

with

$$A = e^{(i/2)\mathbf{q} \cdot \mathbf{r}} + e^{-(i/2)\mathbf{q} \cdot \mathbf{r}} = A^{\dagger}. \quad (5.5)$$

From Eqs. (5.1) and (2.1) follows

$$F(t) = \frac{1}{m_0} \sum_f e^{u(e_f - e)} |\langle \varphi_f | A | \varphi \rangle|^2 = \frac{\langle \varphi | A^{\dagger} e^{it(H-e)} A | \varphi \rangle}{\langle \varphi | A^{\dagger} A | \varphi \rangle}. \quad (5.6)$$

Formally, this can be written as

$$F(t) = \sum_{k=0}^{\infty} \frac{(it)^k}{k!} \frac{m_k}{m_0}. \quad (5.7)$$

A partial summation is achieved in the cumulant expansion, which is again formally,

$$F(t) = \exp \left[\sum_{k=1}^{\infty} \frac{(it)^k}{k!} \lambda_k \right]. \quad (5.8)$$

The obvious connections between the first few cumulants λ_k and the moments m_k are

$$\lambda_1 = \frac{m_1}{m_0}, \quad (5.9)$$

$$\lambda_2 = \frac{m_2}{m_0} - \left[\frac{m_1}{m_0} \right]^2, \quad (5.10)$$

$$\lambda_3 = \frac{m_3}{m_0} - \frac{3m_2 m_1}{m_0^2} + 2 \left[\frac{m_1}{m_0} \right]^3. \quad (5.11)$$

Truncating the expansion at λ_2 yields

$$\begin{aligned}
S(q, \omega) &\approx S_2 \equiv \frac{m_0}{2\pi} \int_{-\infty}^{+\infty} dt e^{-i\omega't} e^{it\lambda_1 - t^2\lambda_2/2} \\
&= \frac{m_0}{(2\pi\lambda_2)^{1/2}} e^{-(\omega' - \lambda_1)^2/2\lambda_2}. \quad (5.12)
\end{aligned}$$

This results in a peak at the location $\omega' = \lambda_1$ with a width $\sqrt{\lambda_2}$. Truncating at λ_3 and expanding in λ_3 yields

$$\begin{aligned}
S(q, \omega) &\approx S_3 \equiv \frac{m_0}{(2\pi\lambda_2)^{1/2}} e^{-(\omega' - \lambda_1)^2/2\lambda_2} \\
&\times \left\{ 1 + \frac{\lambda_3}{6} \frac{\omega' - \lambda_1}{\lambda_2} \left[\left[\frac{\omega' - \lambda_1}{\lambda_2} \right]^2 - \frac{3}{\lambda_2} \right] \right\} \quad (5.13)
\end{aligned}$$

which is peaked at

$$\omega' \approx \lambda_1 - \frac{\lambda_3}{2\lambda_2}. \quad (5.14)$$

In view of the power-law decrease of $\varphi(p)$ the question arises whether higher moments exist at all. One has to know how $S(q, \omega)$ decreases for $\omega \rightarrow \infty$ and q fixed. In our model of Yukawa or exponential interactions we can give an analytical answer which we shall derive now. According to Eq. (2.3) the continuum part of S has the exact form

$$\begin{aligned}
S_C &= \int d\mathbf{p} |\langle \varphi_p^{(+)} | e^{(i/2)\mathbf{q}\cdot\mathbf{r}} + e^{-(i/2)\mathbf{q}\cdot\mathbf{r}} | \varphi \rangle|^2 \frac{m}{2k} \delta(p - k) \\
&= \frac{mk}{2} \int d\hat{\mathbf{p}} |\langle \varphi_{k\hat{\mathbf{p}}}^{(+)} | e^{(i/2)\mathbf{q}\cdot\mathbf{r}} + e^{-(i/2)\mathbf{q}\cdot\mathbf{r}} | \varphi \rangle|^2, \quad (5.15)
\end{aligned}$$

where

$$k = [m(\omega + e) - (q^2/4)]^{1/2} \quad (5.16)$$

increases with ω . A naive estimate for large ω and therefore large k would be to approximate $|\varphi_{k\hat{\mathbf{p}}}^{(+)}\rangle$ by the free state $|k\hat{\mathbf{p}}\rangle$. Based on Eq. (2.14) this would yield the power law $O(1/\omega^{7/2})$; this is incorrect. The estimate has to take into account the orthogonality of $\varphi_p^{(+)}$ and φ . We Galilean transform the scattering state in the form

$$\begin{aligned}
\langle \varphi_p^{(+)} | e^{i\mathbf{q}\cdot\mathbf{r}} &= \langle \mathbf{p} | e^{i\mathbf{q}\cdot\mathbf{r}} + \langle \mathbf{p} | V\tilde{G}^{(-)} e^{i\mathbf{q}\cdot\mathbf{r}} \\
&= \langle \mathbf{p} - \mathbf{q} | + \langle \mathbf{p} - \mathbf{q} | V\tilde{G}^{(-)}. \quad (5.17)
\end{aligned}$$

Here

$$G^{(-)} \equiv \frac{1}{E_p - i\epsilon - H_0(\mathbf{p}) - V} \quad (5.18)$$

and

$$\tilde{G}^{(-)} \equiv \frac{1}{E_p - i\epsilon - H_0(\mathbf{p} + \mathbf{q}) - V}. \quad (5.19)$$

In view of the transformed free state $\langle \mathbf{p} - \mathbf{q} |$, we rewrite $\tilde{G}^{(-)}$ as

$$\begin{aligned}
\tilde{G}^{(-)} &= \frac{1}{E_{\mathbf{p}-\mathbf{q}} - i\epsilon - H + [E_p - E_{\mathbf{p}-\mathbf{q}} + H_0(\mathbf{p}) - H_0(\mathbf{p} + \mathbf{q})]} \\
&\equiv \frac{1}{E_{\mathbf{p}-\mathbf{q}} - i\epsilon - H - a} \quad (5.20)
\end{aligned}$$

with

$$a \equiv \frac{2\tilde{\mathbf{p}}\cdot\mathbf{q}}{m} + \frac{2q^2}{m} - \frac{2\mathbf{p}\cdot\mathbf{q}}{m}. \quad (5.21)$$

The tilde on \mathbf{p} indicates the operator character in contrast to the c number \mathbf{p} . With this preparation we are ready to regard the type of matrix element occurring in Eq. (5.15):

$$\begin{aligned}
M &\equiv \langle \varphi_p^{(+)} | e^{i\mathbf{q}\cdot\mathbf{r}} | \varphi \rangle \\
&= \langle \mathbf{p} - \mathbf{q} | \varphi \rangle + \langle \mathbf{p} - \mathbf{q} | V\tilde{G}^{(-)} | \varphi \rangle. \quad (5.22)
\end{aligned}$$

Using the resolvent identity

$$\tilde{G}^{(-)} = G^{(-)}(E_{\mathbf{p}-\mathbf{q}}) + \tilde{G}^{(-)} a G^{(-)}(E_{\mathbf{p}-\mathbf{q}}), \quad (5.23)$$

we get

$$\begin{aligned}
M &= \langle \mathbf{p} - \mathbf{q} | \varphi \rangle + \langle \mathbf{p} - \mathbf{q} | V G^{(-)}(E_{\mathbf{p}-\mathbf{q}}) | \varphi \rangle \\
&\quad + \langle \mathbf{p} - \mathbf{q} | V \tilde{G}^{(-)} a G^{(-)}(E_{\mathbf{p}-\mathbf{q}}) | \varphi \rangle. \quad (5.24)
\end{aligned}$$

The first two terms combine to obtain

$$\langle \varphi_{\mathbf{p}-\mathbf{q}}^{(+)} | \varphi \rangle = 0 \quad (5.25)$$

and we are left with

$$M = \frac{1}{E_{\mathbf{p}-\mathbf{q}} - e} \langle \mathbf{p} - \mathbf{q} | V \tilde{G}^{(-)} a | \varphi \rangle. \quad (5.26)$$

Now we use

$$\begin{aligned}
\tilde{G}^{(-)} a &= [\tilde{G}^{(-)}, a] + a \tilde{G}^{(-)} \\
&= \tilde{G}^{(-)} [V, 2\tilde{\mathbf{p}}\cdot\mathbf{q}/m] \tilde{G}^{(-)} + a \tilde{G}^{(-)}, \quad (5.27)
\end{aligned}$$

and note that

$$a | \mathbf{p} - \mathbf{q} \rangle = \left[\frac{2(\mathbf{p} - \mathbf{q})\cdot\mathbf{q}}{m} + \frac{2q^2}{m} - \frac{2\mathbf{p}\cdot\mathbf{q}}{m} \right] | \mathbf{p} - \mathbf{q} \rangle = 0. \quad (5.28)$$

This allows us to put

$$\langle \mathbf{p} - \mathbf{q} | V a = \langle \mathbf{p} - \mathbf{q} | [V, a]. \quad (5.29)$$

All this together with another application of Eq. (5.23) yields

$$M = \frac{1}{(E_{\mathbf{p}-\mathbf{q}} - e)^2} \langle \mathbf{p} - \mathbf{q} | [V, a] | \varphi \rangle + \dots \quad (5.30)$$

to leading order for $|\mathbf{p}| \rightarrow \infty$.

The estimate of the matrix element is done most easily in configuration space:

$$\begin{aligned}
M_0 \equiv \langle \mathbf{p}-\mathbf{q} | [V, a] | \varphi \rangle &= \frac{1}{(2\pi)^{3/2}} \int d\mathbf{r} e^{-i(\mathbf{p}-\mathbf{q})\cdot\mathbf{r}} \frac{2i\mathbf{q}\cdot\hat{\mathbf{r}}}{m} V'(r) \varphi(r) \\
&= -\frac{4\pi}{(2\pi)^{3/2}} \frac{2}{m} \frac{(\mathbf{p}-\mathbf{q})\cdot\mathbf{q}}{|\mathbf{p}-\mathbf{q}|} \int_0^\infty dr r^2 j_1(|\mathbf{p}-\mathbf{q}|r) V'(r) \varphi(r).
\end{aligned} \tag{5.31}$$

We use the integral representation

$$j_1(z) = -\frac{i}{2} \int_{-1}^{+1} dt t e^{izt} P_1(t) \tag{5.32}$$

and

$$|\mathbf{p}-\mathbf{q}| \xrightarrow{p \rightarrow \infty} p - \hat{\mathbf{p}}\cdot\mathbf{q}, \tag{5.33}$$

and can rewrite the integral in Eq. (5.31) as

$$\begin{aligned}
-\frac{i}{2} \int_{-1}^{+1} dt t \int_0^\infty dr r^2 e^{i(p-\hat{\mathbf{p}}\cdot\mathbf{q})tr} V'(r) \varphi(r) &= -\frac{i}{2} \int_{-1}^{+1} dt t \left[\frac{e^{ipt}}{ipt} e^{-i\hat{\mathbf{p}}\cdot\mathbf{q}tr} [r^2 V'(r)] \varphi(r) \Big|_0^\infty \right. \\
&\quad \left. - \frac{1}{ipt} \int_0^\infty dr e^{iptr} \frac{\partial}{\partial r} \{ e^{-i\hat{\mathbf{p}}\cdot\mathbf{q}tr} [r^2 V'(r)] \varphi(r) \} \right] \\
&= \frac{1}{p} [r^2 V'(r)]|_{r=0} \varphi(r=0) + O\left[\frac{1}{p^2}\right].
\end{aligned} \tag{5.34}$$

The coefficient of $1/p$ is different from zero for Yukawa interactions. Finally we expand the factor in front of the integral in Eq. (5.31) and the denominator in Eq. (5.30) and end up with

$$M \rightarrow -\frac{2m}{p^5} \frac{4\pi}{(2\pi)^{3/2}} (r^2 V'(r))|_{r=0} \varphi(r=0) \left[\hat{\mathbf{p}}\cdot\mathbf{q} - \frac{q^2}{p} \right] \left[1 + \frac{5\hat{\mathbf{p}}\cdot\mathbf{q}}{p} \right]. \tag{5.35}$$

Then going back to Eq. (5.15) we find

$$\begin{aligned}
S_C(q, \omega) &\rightarrow \frac{m^3}{2k^{11}} \frac{16\pi^2}{(2\pi)^3} \{ [r^2 V'(r)]|_{r=0} \varphi(r=0) \}^2 \int d\hat{\mathbf{p}} [5(\hat{\mathbf{p}}\cdot\mathbf{q})^2 - q^2]^2 \\
&= \frac{32}{3} \frac{q^4}{m^{5/2}} \{ [r^2 V'(r)]|_{r=0} \varphi(r=0) \}^2 \frac{1}{\omega^{11/2}} \equiv C \frac{q^4}{\omega^{5.5}}
\end{aligned} \tag{5.36}$$

for $\omega \rightarrow \infty$.

In the case of the one charged particle the decrease is one power less:

$$S(q, \omega) \rightarrow \frac{q^2}{3m^{3/2}} \{ [r^2 V'(r)]|_{r=0} \varphi(r=0) \}^2 \frac{1}{\omega^{4.5}}. \tag{5.37}$$

It is interesting to note that in Ref. 7 an exponential decrease has been assumed which is in conflict with that analytical result.

An immediate consequence of that power law is the nonexistence of the moments m_k for $k \geq 5$, for two charged particles, and $k \geq 4$ for one charged particle. This rules out the expansions (5.7) and (5.8) and throws doubts on the quantitative usefulness of the low order approximations (5.12) and (5.13).

From Eq. (5.1) it follows that

$$F^{(n)}(t)|_{t=0} = \frac{1}{m_0} \int_0^\infty d\omega' (i\omega')^n S(q, \omega) \tag{5.38}$$

which exists up to $n=4$ in the case of two charged particles. Therefore, putting

$$F(t) \equiv \sum_{n=0}^4 \frac{t^n}{n!} F^{(n)}(0) + f(t) \tag{5.39}$$

it is easy to see that

$$f(t) \rightarrow \text{const} t^{4+1/2} \tag{5.40}$$

for $t \rightarrow 0$ and that it is therefore not analytic at $t=0$. In Sec. VI we shall see indirectly the quantitative importance of $f(t)$. In doing that one has to determine the few low order moments. This is straightforward following Refs. 2 and 5 with the results

$$m_0 = \langle \varphi | A^\dagger A | \varphi \rangle = 2 + 2 \langle \varphi | e^{iq \cdot r} | \varphi \rangle, \quad (5.41)$$

$$m_1 = \langle \varphi | A^\dagger (H - e) A | \varphi \rangle = \frac{1}{2} \langle \varphi | [A^\dagger, [H, A]] | \varphi \rangle = \frac{q^2}{2m} (1 - \langle \varphi | e^{iq \cdot r} | \varphi \rangle), \quad (5.42)$$

$$m_2 = \langle \varphi | A^\dagger (H - e)^2 A | \varphi \rangle = \langle \varphi | [A^\dagger, H][H, A] | \varphi \rangle \\ = \frac{q^4}{8m^2} + \frac{2q^2}{3m} \langle H_0 \rangle - \frac{3q^4}{8m^2} \langle \varphi | e^{iq \cdot r} | \varphi \rangle + \frac{2q^3}{m^2} \langle \varphi | p_{\parallel} e^{iq \cdot r} | \varphi \rangle - \frac{2q^2}{m^2} \langle \varphi | p_{\parallel}^2 e^{iq \cdot r} | \varphi \rangle, \quad (5.43)$$

and

$$m_3 = \langle \varphi | A^\dagger (H - e)^3 A | \varphi \rangle = \frac{1}{2} \langle \varphi | [[A^\dagger, H], [H, [H, A]]] | \varphi \rangle \\ = \frac{q^6}{32m^3} + \frac{q^4}{2m^2} \langle H_0 \rangle + \frac{3q^6}{32m^3} \langle \varphi | e^{iq \cdot r} | \varphi \rangle - \frac{q^5}{2m^3} \langle \varphi | p_{\parallel} e^{iq \cdot r} | \varphi \rangle + \frac{q^4}{2m^3} \langle \varphi | p_{\parallel}^2 e^{iq \cdot r} | \varphi \rangle \\ = \frac{q^2}{3m^2} \langle \Delta V \rangle + \frac{q^2}{m^2} \langle \varphi | [p_{\parallel}, [p_{\parallel}, V]] e^{iq \cdot r} | \varphi \rangle. \quad (5.44)$$

The cumulants follow from Eq. (5.9)–(5.11). For $q \rightarrow \infty$ the interference terms are negligible and one gets

$$\lambda_1 \xrightarrow{q \rightarrow \infty} \frac{q^2}{4m}, \quad (5.45)$$

$$\lambda_2 \xrightarrow{q \rightarrow \infty} \frac{q^2}{3m} \langle H_0 \rangle, \quad (5.46)$$

$$\lambda_3 \xrightarrow{q \rightarrow \infty} \frac{q^2}{6m^2} \langle \Delta V \rangle. \quad (5.47)$$

In the case of the one charged “nucleon” one has, instead of Eq. (5.5),

$$A = e^{(i/2)q \cdot r} \neq A^\dagger \quad (5.48)$$

and it is easy to see that in this case equal signs in expressions (5.45)–(5.47) are valid. Also note that for $q \rightarrow \infty$, the cumulants are independent of the charge of the target.

VI. NUMERICAL RESULTS

The two “nucleons” interact by the local potentials (2.11) or (2.12), which support one bound state φ with energy $e = -2.23$ MeV. For the parameters of V in Eq. (2.11) we refer to Ref. 4; the parameters of V in Eq. (2.12) are $V_0 = -0.8150$ fm⁻¹ and $\mu = 1.35$ fm⁻¹. They are adjusted such that V of Eq. (2.12) has the same $\langle H_0 \rangle = 10.8$ MeV as V of Eq. (2.11). $\varphi(p)$ is determined numerically via

$$\varphi(p) = \frac{1}{e - (p^2/m)} \int_0^\infty dp' p'^2 V_0(p, p') \varphi(p'), \quad (6.1)$$

where $V_0(p, p')$ are the well known s -wave momentum representations of Eqs. (2.11) and (2.12). Since the asymptotic behavior [Eq. (2.14)] is important for all our estimates we display it in Table I for the potential MT III of Eq. (2.11).

The final-state interaction is driven by the two-body T matrix [Eq. (2.7)], which obeys the Lippmann-Schwinger equation

$$T(p, k, t) = V(p, k, t)$$

$$+ \int d\mathbf{p}' V(p, p', \tilde{t}) \frac{1}{E_k + i\epsilon - E_{p'}} T(p', k, t'), \quad (6.2)$$

where

$$t = \hat{\mathbf{p}} \cdot \hat{\mathbf{k}}, \quad (6.3)$$

$$t' = \hat{\mathbf{p}}' \cdot \hat{\mathbf{k}}, \quad (6.4)$$

and

$$\tilde{t} = \hat{\mathbf{p}} \cdot \hat{\mathbf{p}}' = tt' + (1 - t^2)^{1/2} (1 - t'^2)^{1/2} \cos(\phi - \phi'). \quad (6.5)$$

For a Yukawa interaction $V = V_0 e^{\mu r} / r$,

$$V(p, p', t) = \frac{V_0 / 2\pi^2}{p^2 + p'^2 - 2pp't + \mu^2}, \quad (6.6)$$

and the ϕ' integral in Eq. (6.2) can be performed analytically:

TABLE I. Bound-state wave function $\varphi(p)$ for the potential (2.11) and its asymptotic behavior.

p (fm ⁻¹)	$\varphi(p)$ (fm ^{3/2})	$\varphi(p)p^4$ (fm ^{-5/2})
10.0	-0.400×10^{-4}	-0.400
20.0	-0.170×10^{-5}	-0.269
30.0	-0.312×10^{-6}	-0.252
40.0	-0.967×10^{-7}	-0.248
50.0	-0.393×10^{-7}	-0.246
100.0	-0.243×10^{-8}	-0.243
200.0	-0.151×10^{-9}	-0.242

$$v(p, p', t, t') \equiv \int_0^{2\pi} d\phi' V(p, p', \bar{t})$$

$$= \frac{V_0/\pi}{[(p^2 + p'^2 + \mu^2 - 2pp'tt')^2 - 4p^2p'^2(1-t^2)(1-t'^2)]^{1/2}} \quad (6.7)$$

Then the two-dimensional integral equation for T to be solved is

$$T(p, k, t) = V(p, k, t) + \int_0^\infty dp' p'^2 \frac{1}{(k^2/m) + i\epsilon - (p'^2/m)} \int_{-1}^{+1} dt' v(p, p', t, t') T(p', k, t'). \quad (6.8)$$

Following Ref. 8 one avoids complex arithmetic and defines the K matrix by

$$K(p, k, t, t_0) = \frac{1}{2\pi} v(p, k, t, t_0) + \int_0^\infty dp' p'^2 \frac{P}{E_k - E_{p'}} \int_{-1}^{+1} dt' v(p, p', t, t') K(p', k, t', t_0). \quad (6.9)$$

Therefore, the half-shell T matrix is given by quadrature:

$$T(p, k, t) = K(p, k, t, 1) - m\pi^2 ki \int_{-1}^{+1} dt' K(p, k, t, t') T(k, k, t'). \quad (6.10)$$

This requires the knowledge of the on-shell T matrix which apparently is given through the one-dimensional integral equation

$$T(k, k, t) = K(k, k, t, 1) - m\pi^2 ki \int_{-1}^{+1} dt' K(k, k, t, t') T(k, k, t'). \quad (6.11)$$

In studying the approach to scaling we shall need high energy and momentum transfers which, via Eq. (2.10), can lead to large initial momenta k . For those values the T matrix is strongly peaked in the forward direction $t \approx 1$ as we illustrate in Fig. 1. Clearly a representation of T by a small number of partial waves would be totally unjustified. In solving the two-dimensional equation (6.8), one is free from that defect. Typical numbers of Gaussian quadrature points are $N_p = 60$ and $N_t = 30$,

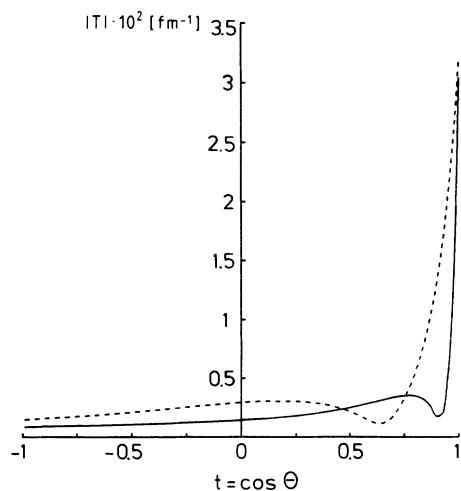


FIG. 1. Magnitude of the on-shell two-body T matrix for the potential (2.11) against $t = \cos \theta$ at $k = 2.5 \text{ fm}^{-1}$ (dashed curve) and $k = 5.0 \text{ fm}^{-1}$ (solid curve).

where the t values should be concentrated near $t = 1$.

Having φ and T at one's disposal one can perform the fourfold integral (2.8) for the continuum part S_C of the structure function. We apply Gaussian quadratures throughout and determine $S_C(q, \omega)$ within four digits near the maximum of the quasielastic peak and with less accuracy for the greatest η values which contribute only at the fourth digit in the sum rule (3.23). These are our pseudodata. We show in Fig. 2 the structure function S_C for various q 's as a function of $\eta = 2m\omega/q^2$. If one multiplies S_C by $q^2/4m$ one neatly sees the typical sequence of functions approaching a δ function. This is displayed in Fig. 3.

Let us now illustrate in Table II the evaluation of the sum rules (3.21)–(3.23) with our pseudodata. For (3.21) and (3.22) the left-hand sides are shown and for Eq. (3.23) the expectation value “ $\langle H_0 \rangle$ ” assuming an equal sign. In the last column η_{\max} is the cutoff value for the integral in Eq. (3.23) which guarantees the extraction of “ $\langle H_0 \rangle$ ” within four digits. We see that except for $q = 2.5 \text{ fm}^{-1}$ the extraction of “ $\langle H_0 \rangle$ ” works very well. At $q = 2.5 \text{ fm}^{-1}$ the contribution to $\langle H_0 \rangle$ from the elastic channel (+2.2 MeV) and the interference terms (−1.2 MeV) are

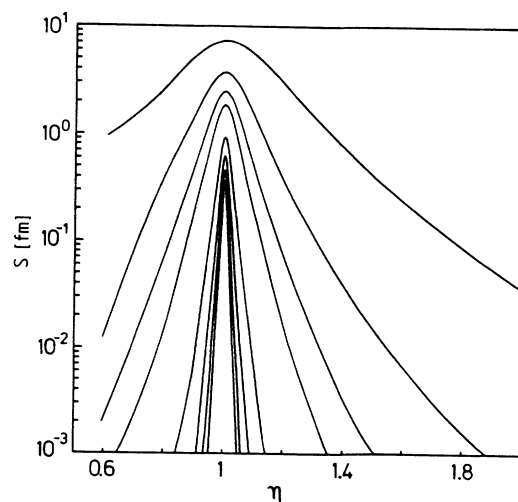


FIG. 2. Structure function S for the potential (2.11) against η . The curves counted from top to bottom belong to $q = 2.5, 5.0, 7.5, 10.0, 20.0, 30.0, 40.0,$ and 50.0 fm^{-1} , respectively.

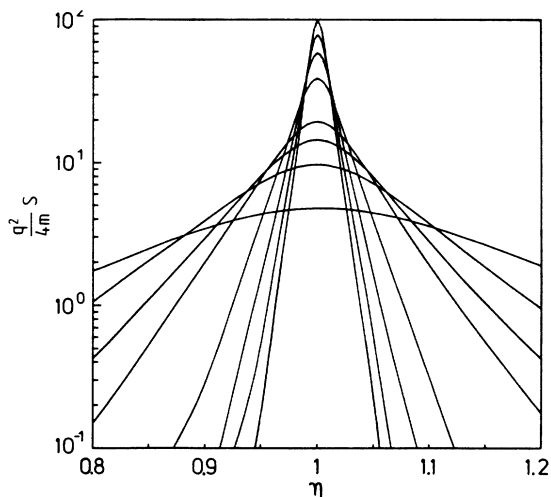


FIG. 3. The quantity $(q^2/4m)S$ for the potential (2.11) against η . The same q values as in Fig. 2, now counted in reverse order in the maxima.

responsible for the deviation from 10.8 MeV. Both contributions are of equal magnitude. In the case of the regular and purely attractive potential [Eq. (2.12)] the approach towards the asymptotic value is faster as shown in Table III.

Experimentally, the structure function is increasing again on the right-hand side of the quasielastic peak due to isobar excitations and other processes, which are not taken into account in our model. Therefore, we ask how well can one extract $\langle H_0 \rangle$ alone from the left wing of the peak. In other words, we replace the integral in Eq. (3.23) by twice the integral from η_{\min} to 1. Table IV shows the results. We see that only around $q \sim 7 \text{ fm}^{-1}$ do we come into an acceptable neighborhood of the actual value.

We mention that in the case of one charged particle the sum rule

$$\frac{q^2}{2m} \int_{\eta_{\min}}^{\infty} d\eta (\eta - 1)^2 S(q, \eta) = \frac{4m}{3q^2} \langle H_0 \rangle - \frac{1}{4} |\langle \varphi | e^{(i/2)q \cdot r} | \varphi \rangle|^2 \quad (6.12)$$

TABLE II. Sum rules (3.21)–(3.23) for the potential (2.11) for various momentum transfers q . The last row displays the exact values. η_{\max} are the cutoff values necessary to evaluate Eq. (3.23) within four digits.

q (fm^{-1})	Sum rule [Eq. (3.21)]	Sum rule [Eq. (3.22)]	$\langle H_0 \rangle$ (MeV) [Eq. (3.23)]	η_{\max}
2.5	0.97	0.02	9.84	40
5.0	1.00	0.00	10.6	30
7.5	1.00	0.00	11.1	30
10.0	1.00	0.00	11.1	30
20.0	1.00	0.00	10.9	12
30.0	1.00	0.00	10.8	12
40.0	1.00	0.00	10.8	10
50.0	1.00	0.00	10.8	10
∞	1.00	0.00	10.8	

is an exact identity. Here we added explicitly the correction term linked to the elastic form factor, which dies out quickly with q . This relation was a useful numerical test, which turned out to be fulfilled within three digits.

If one neglects that correction term in the spirit of the model-independent extraction of $\langle H_0 \rangle$, one only gets $\langle H_0 \rangle = 9.71 \text{ MeV}$ at $q = 2.5 \text{ fm}^{-1}$, whereas already at $q = 5.0 \text{ fm}^{-1}$ the correction term can be neglected. Therefore, in Table II we see that at $q = 2.5 \text{ fm}^{-1}$ the contribution from the elastic channel is important. In the case of the deuteron this correction term can be taken from the elastic form factor and therefore $\langle H_0 \rangle$ can be extracted from the structure function for *all* q values. For $q \geq 5 \text{ fm}^{-1}$, where the interference terms are negligible, we expect a similar ξ scaling behavior for ${}^3\text{He}$ and the deuteron. Taking only the left wing of the quasielastic peak into account, the extraction of $\langle H_0 \rangle$ is less favorable. For $q = 2.5, 5.0,$ and 10 fm^{-1} one gets $\langle H_0 \rangle = 6.21, 9.61,$ and 10.2 MeV , respectively, neglecting the correction term.

Let us now regard y scaling in some detail. The scaling limit is the longitudinal momentum distribution $P_L(y)$, which we display for our model in Fig. 4. Up to $y \approx \pm 2 \text{ fm}^{-1}$ the decrease is roughly exponential, then the zero of $\varphi(p)$ causes the shoulder. In a more realistic deuteron model the d -wave admixture fills that dip.⁹ At much larger values, however, the decrease has to go over into a power law. In our model, as follows from Eqs. (4.5) and (2.14), the decrease is asymptotically $O(1/y^6)$, which roughly starts at $y = 30 \text{ fm}^{-1}$ according to Table I.

As we saw in Sec. IV the leading correction term (4.8) to the y scaling is the same in both cases, one or two charged “nucleons.” Beyond that the first interference term (4.6) is of fourth order in $1/q$. Therefore the y -scaling behavior is the same in both cases and we discuss only two charged “nucleons.”

Now Fig. 5 displays our pseudodata $(q/2m)S$ for different q values against y in comparison with the asymptotic limit $P_L(y)$. A rough glimpse tells that there is scaling to the right values for $-1.5 \text{ fm}^{-1} \leq y \leq 1 \text{ fm}^{-1}$ and $q > 5 \text{ fm}^{-1}$. For y values outside that interval, scaling is not yet reached for the rather large q values shown. For $q \leq 10 \text{ fm}^{-1}$, the left wing pseudodata scale in the full interval shown—but *not* to the correct function. This is

TABLE III. Same as in Table II for the exponential potential (2.12).

q (fm $^{-1}$)	Sum rule [Eq. (3.21)]	Sum rule [Eq. (3.22)]	$\langle H_0 \rangle$ (MeV) [Eq. (3.23)]	η_{\max}
2.5	0.98	0.02	10.1	35
5.0	1.00	0.00	11.0	30
7.5	1.00	0.00	10.9	30
10.0	1.00	0.00	10.8	20
20.0	1.00	0.00	10.8	20
∞	1.00	0.00	10.8	

apparently a dangerous situation, since the scaling behavior of the (pseudo)data could be misinterpreted as representing the momentum distribution. A look at higher q values reveals that the pseudodata for $q=20$ fm $^{-1}$ make a move in the direction of the limit function. The convergence towards that function is, however, very slow as we have seen by evaluating the pseudodata for $q=30-50$ fm $^{-1}$. Therefore, our numerical experience indicates that the limit in q is not uniform in y . One can see this in the extreme case for fixed q and $y \rightarrow \infty$. Then according to Eqs. (4.5) and (2.14), $P_L(y) = O(1/y^6)$. In that limit $\omega = O(y)$ and $q/2mS(q, \omega) = O(1/\omega^{5.5})$ or $O(1/\omega^{4.5})$ for two or one charged particles, respectively, according to Eqs. (5.36) and (5.37). Thus the scaling function is above $P_L(y)$. We think that this tendency is already visible on the right slope of Fig. 5. We would, however, like to emphasize that for fixed y and $q \rightarrow \infty$, $(q/2m)S$ has finally to converge to $P_L(y)$ for the potentials considered by us. They include superpositions of Yukawa interactions which are typical for nuclear physics. It remains to be seen in how far that slow approach gets modified in a fully relativistic treatment.

A more quantitative insight can be drawn from Fig. 6, where we display the pseudodata $(q/2m)S$ for various fixed y 's against q . Note that y is limited from below by

$$y_{\min} = \frac{q}{2}(\eta_{\min} - 1) = -\frac{q}{4} - \frac{me}{q}. \quad (6.13)$$

Besides the asymptotic value $P_L(y)$ 10% and 30% deviations are also shown. Note that even at $y=0$, right in the quasielastic peak, and $q=1$ fm $^{-1}$, one is more than 30% off. Clearly within the interval 10 fm $^{-1} \leq q \leq 50$ fm $^{-1}$ the

pseudodata $(q/2m)S$ do not scale, but move slowly towards the asymptotic value $P_L(y)$. In that q interval and for -1.25 fm $^{-1} \leq y \leq 0.5$ fm $^{-1}$ the pseudodata remain within 10% of the asymptotic value, whereas outside that y interval the deviations are larger. It is also very interesting to see the varying approach towards $P_L(y)$ for different y 's and smaller q 's, which bares interesting information on the interplay of φ and the half-shell T matrix.

For the very regular potential (2.12) the approach towards y scaling with the correct limit is faster as shown in Fig. 7. Note the change of slope for $y \leq -0.75$ fm $^{-1}$ in comparison to Fig. 6. This shows that indeed the structure function depends sensitively on the properties of the underlying interaction.

Let us comment on the importance of the final-state interaction in the evaluation of S . Let S_0 be the structure function putting $T=0$ in Eq. (2.8). We compare in Fig. 8 $(q/2m)S$ and $(q/2m)S_0$ for fixed q values against y . We see a significant difference between the two curves for negative and positive y 's. The difference is essentially odd in y , which can be easily inferred from Eq. (4.2) in first order in V and large q values. Also shown is $P_L(y)$ and clearly the approximate structure function $(q/2m)S_0$ deviates more strongly from $P_L(y)$ than the correct one including final-state interactions. The pseudodata are rather badly described by S_0 on the left wing, where the analysis of real data is especially of interest in terms of nucleonic degrees of freedom and $(q/2m)S_0$ falls below the values of the momentum distribution.

The difference between S and S_0 is very much visible in the asymptotic behavior in ω for fixed q . It is easily seen from the exact form

TABLE IV. Same as in Table II but using only the left wing of the quasielastic peak.

q (fm $^{-1}$)	Sum rule [Eq. (3.21)]	Sum rule [Eq. (3.22)]	$\langle H_0 \rangle$ (MeV) [Eq. (3.23)]
2.5	0.93	0.00	6.23
5.0	1.00	0.00	8.43
7.5	1.00	0.00	10.1
10.0	1.00	0.00	10.5
20.0	1.00	0.00	10.6
30.0	1.00	0.00	10.6
40.0	1.00	0.00	10.6
50.0	1.00	0.00	10.7
∞	1.00	0.00	10.8

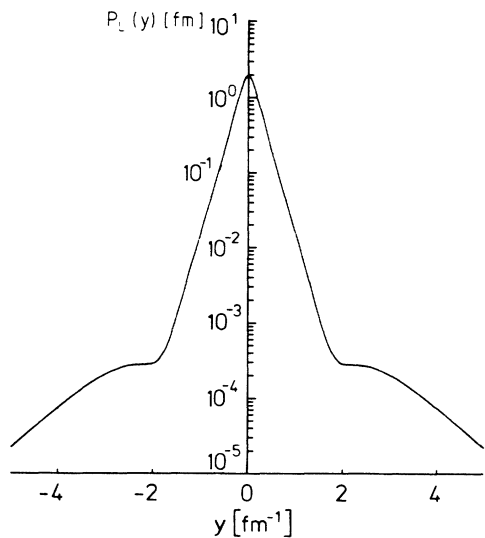


FIG. 4. Longitudinal momentum distribution $P_L(y)$ in the target bound state φ for the potential (2.11).

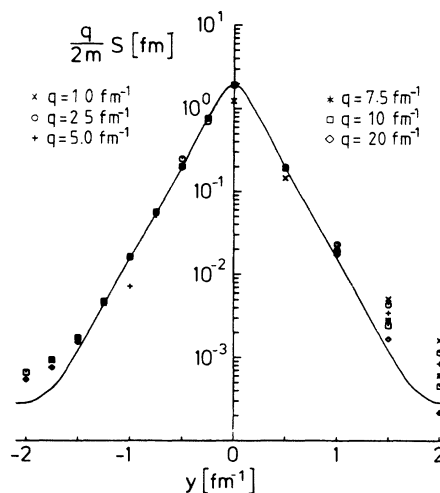


FIG. 5. Scaling function $(q/2m)S$ for various q 's in comparison to its asymptotic limit $P_L(y)$ for $q \rightarrow \infty$.

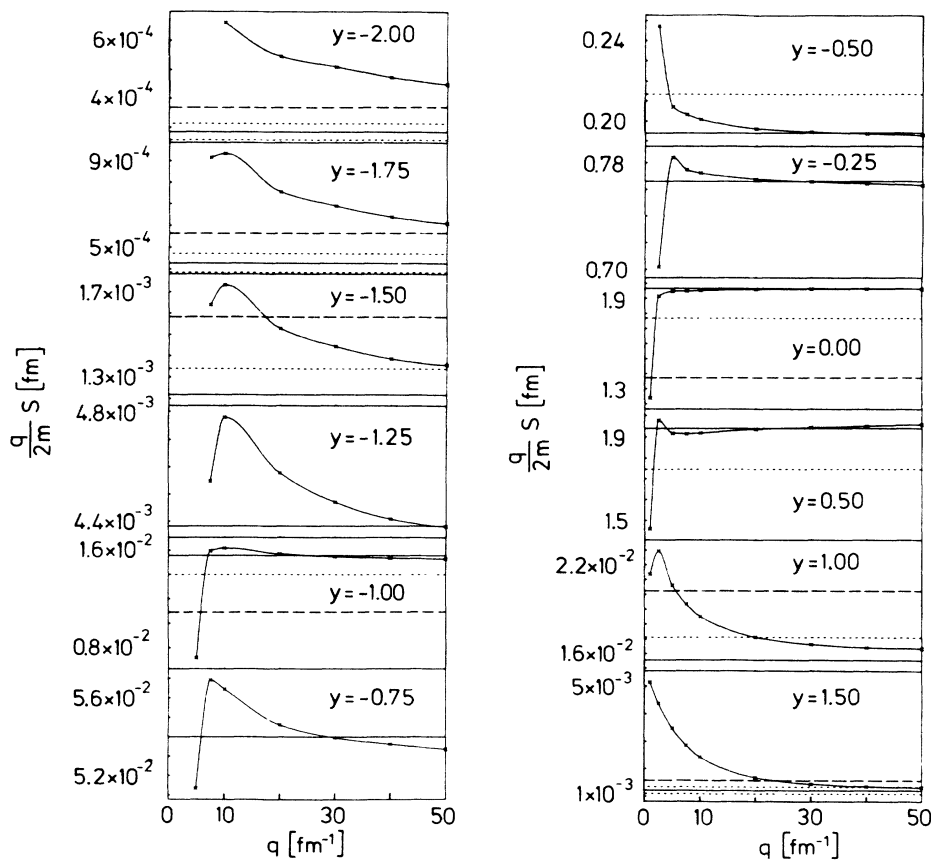


FIG. 6. Scaling function $(q/2m)S$ against q for various fixed y 's. The potential is from Eq. (2.11). The dashed (dotted) lines denote 30% (10%) deviations from the asymptotic value $P_L(y)$ shown by a horizontal solid line.

$$S_0 = \pi m k \int_{-1}^{+1} dt \left| \varphi \left[\left(k^2 + \frac{q^2}{4} - kqt \right)^{1/2} \right] + \varphi \left[\left(k^2 + \frac{q^2}{4} + kqt \right)^{1/2} \right] \right|^2 \quad (6.14)$$

with k given by Eq. (2.10), that

$$S_0 = O \left(\frac{1}{\omega^{7/2}} \right) \quad (6.15)$$

independent of q while

$$S = O \left(\frac{q^4}{\omega^{11/2}} \right). \quad (6.16)$$

The neglect of the final-state interactions is not only unjustified in the left wing of the quasielastic peak, where one finally approaches elastic scattering and where obviously final-state interactions are needed, but also at large energy transfers in the right wing of the quasielastic peak. It is only justified in the peak and its immediate neighborhood that the final-state interaction can be neglected.

Though our model neglects spin degrees of freedom in the NN interaction and is strictly nonrelativistic, our pseudodata qualitatively show features also present in real data. In Ref. 10 a "scaling function" is introduced

which in the nonrelativistic limit coincides with our reduced structure function $(q/2m)S(q, \omega)$, including the definition of y . In Fig. 1 of Ref. 10 experimental data for the scaling function are shown which for $y \leq -200$ MeV/c drop with increasing q values and have a tendency to flatten out at the largest q values ($q \sim 12-14 \text{ fm}^{-1}$) shown. The decrease with q is a clear signature¹⁰ for the presence of final-state interactions. Qualitatively, our Fig. 6 shows a similar behavior and also stresses the importance of final-state interactions. It may be interesting to point out that for a plane-wave approximation the approach towards the asymptotic limit is from below.¹⁰ This however does not mean that this argument can be reversed and an approach from below indicates a weak or negligible final-state interaction. Figure 7 is a clear counterexample of this.

Figure 2 of Ref. 11 is another example where experimental data for the "scaling function" are displayed and which show a striking qualitative similarity to our Fig. 5. Again this definition (Definition I) coincides with ours in the nonrelativistic limit. For $y < -0.2$ GeV/c and the momentum transfer considered, a substantial scale breaking is present, which in our model, results from final-state interaction effects. This stresses the importance of properly including the interacting continuum. Also in our model-study a partial-wave decomposition of that continuum would have been totally inadequate (see Fig. 1).

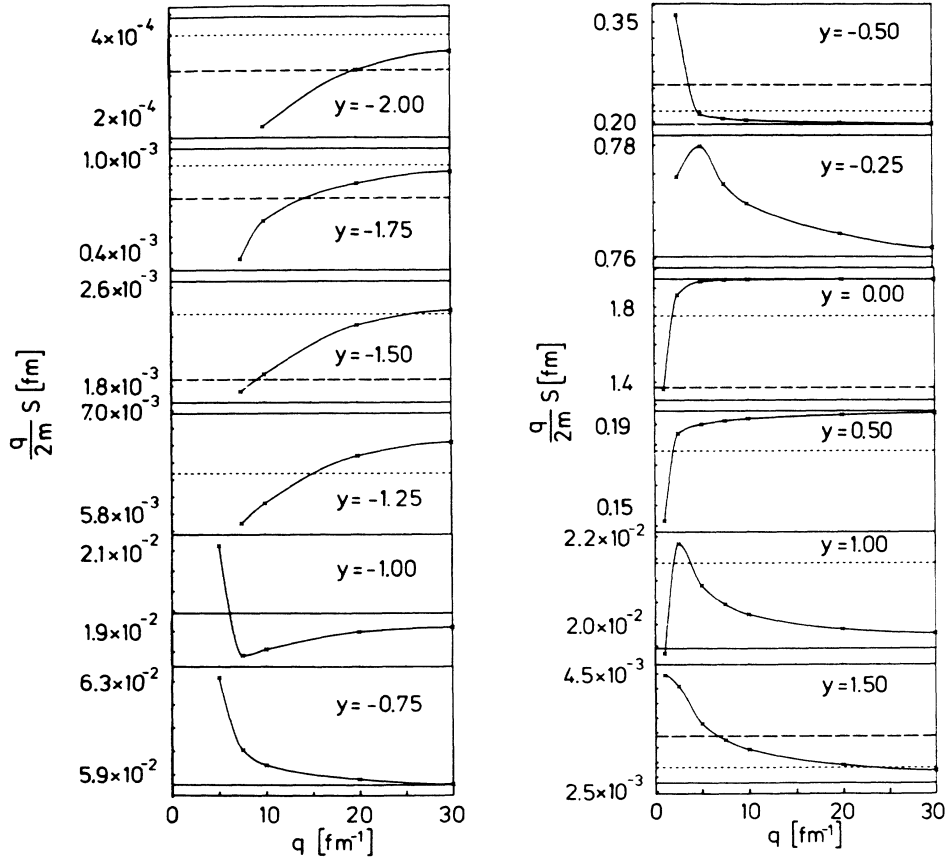


FIG. 7. Same as in Fig. 6 for the potential from Eq. (2.12).

TABLE V. The first three cumulants for the potential (2.11) for various q 's.

q (fm^{-1})	λ_1	λ_2	λ_3
2.5	0.330	0.0308	-0.00465
5.0	1.33	0.181	-0.328
7.5	2.96	0.269	-0.148
10.0	5.25	0.407	0.388
20.0	21.0	1.54	1.55

We finally investigate the possibility to represent the structure functions S by a few cumulants. The first three cumulants for the interaction (2.11) are displayed in Table V. This includes the interference terms. In Table VI we show these cumulants without interference terms, corresponding to the asymptotic forms, Eqs. (5.45)–(5.47). The importance of the interference terms for the cumulants grows with increasing order. For λ_3 even the sign is influenced by the interference terms for

TABLE VI. Same as in Table V neglecting the interference terms.

q (fm^{-1})	λ_1	λ_2	λ_3
2.5	0.328	0.0240	0.0222
5.0	1.31	0.0959	0.0886
7.5	2.96	0.216	0.199
10.0	5.25	0.383	0.354
20.0	21.0	1.53	1.42

lower q values. According to Eq. (5.14) this determines the position of the maximum to be left or right of $\eta=1$. We compare in Fig. 9 the exact S with the approximate S_2 and S_3 of Eqs. (5.12) and (5.13) for two q values. The discrepancy is drastic in height and width. S_3 even shifts the position of the peak. This clearly indicates that the t dependence in Eq. (5.39), beyond the few low-order terms, is important. The inadequacy of S_2 , for instance, can also be seen in the following manner. One can fit S_2 to the pseudodata which provides fits to λ_1 and λ_2 . The

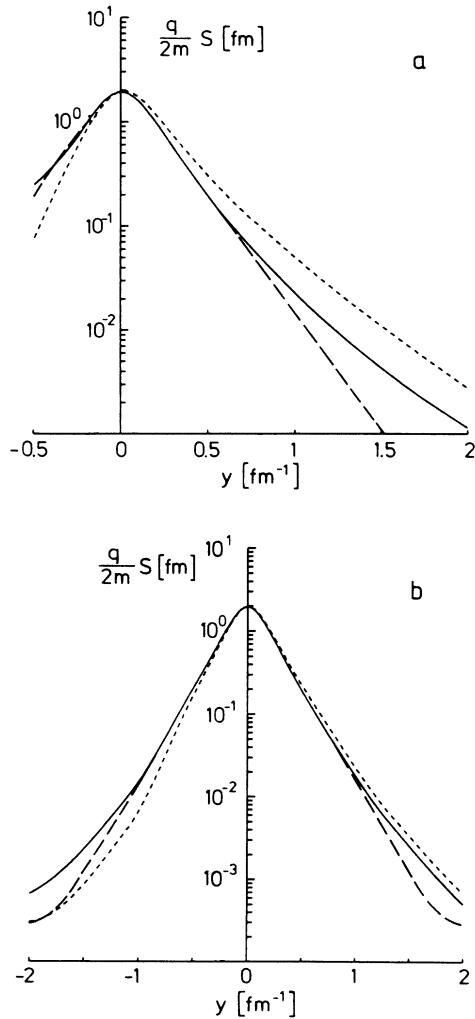


FIG. 8. Comparison of the structure function $(q/2m)S$ (solid curve) with $(q/2m)S_0$ (short-dashed curve) and $P_L(y)$ (long-dashed curve) at (a) $q = 2.5 \text{ fm}^{-1}$ and (b) $q = 10.0 \text{ fm}^{-1}$.

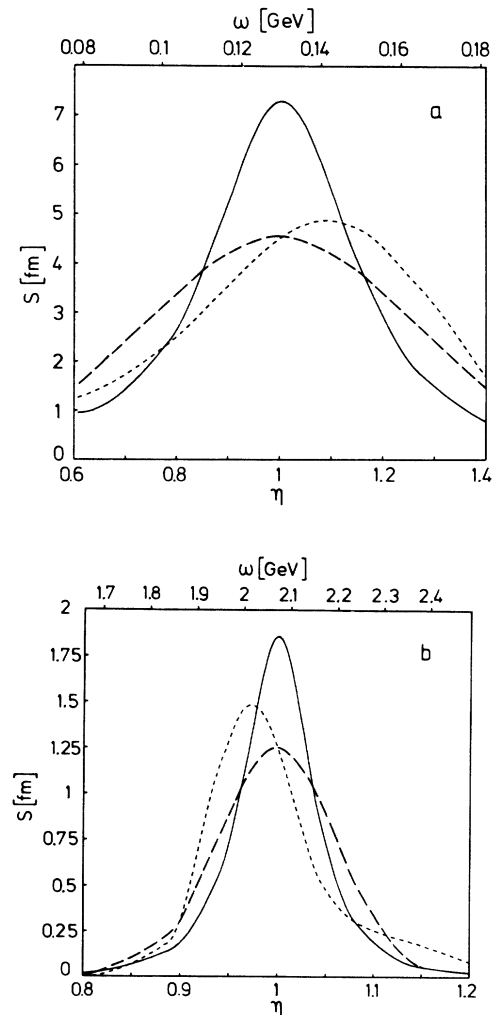


FIG. 9. Comparison of the structure function S (solid curve) with S_2 (long-dashed curve) and S_3 (short-dashed curve) against η or ω for (a) $q = 2.5 \text{ fm}^{-1}$ and (b) $q = 10.0 \text{ fm}^{-1}$.

TABLE VII. $\langle H_0 \rangle$ extracted from Eq. (5.46) and the fit values λ_2 .

q (fm $^{-1}$)	$\langle H_0 \rangle$ (MeV)
2.5	5.40
5.0	5.25
7.5	5.22
10.0	5.19
20.0	5.15
30.0	5.14
40.0	5.13
50.0	5.13

asymptotic values of λ_1 and λ_2 are known theoretically [see Eqs. (5.45) and (5.46)]. In our model these asymptotic limits are reached around $q \approx 10$ fm $^{-1}$. Using the fit values λ_2 and interpreting them according to Eq. (5.46), one can “gain” expectation values of the kinetic energy in the target which are displayed in Table VII. They neatly get independent of q but deviate strongly from the correct value $\langle H_0 \rangle = 10.8$ MeV. We conclude that within our model study the low-order cumulant representation is not useful.

VII. SUMMARY

In a strictly nonrelativistic model the (longitudinal) structure function for quasielastic scattering on a model “nucleus” has been investigated. The model consists of two “nucleons,” which are either both charged or where only one is charged and which interact by local spin independent forces. We have chosen the NN potential MT III, now acting in *all* partial waves, and a purely exponential potential. The final-state interaction is taken into account exactly by evaluating the two-body T matrix directly in three-dimensional space. The numerically precise values for the structure function served as pseudodata to study sum rules, y scaling, the cumulant expansion, and last but not least the importance of the final-state interaction. One of the sum rules delivers the expectation value of the kinetic energy $\langle H_0 \rangle$ in the target ground state. We looked into the question of whether the left wing of the quasielastic peak can be used alone to extract $\langle H_0 \rangle$. It has to be seen in how far the definite results for our model will be modified by a full relativistic treatment. Our results for y scaling, however, show features, which are qualitatively also seen in real data analysis.^{10,11} For small negative y values our pseudodata scale neatly to the

correct limit function $P_L(y)$, the longitudinal momentum distribution, whereas, for larger $|y|$ values the scaling function decreases with increasing q 's and approaches $P_L(y)$ from above (in the case of Malfliet-Tjon potential). For these large negative y values and a certain range of q values, the scaling is badly violated. In our case the deviation from the asymptotic limit is a result of final-state-interaction effects, which stresses the importance of properly treating the interacting continuum. More specifically, our model study showed that y scaling to the correct limit function $P_L(y)$ occurred only for $-1.5 \leq y \leq 1.0$ fm $^{-1}$ and is badly violated for smaller (or larger) values for the numerically studied momentum transfers. The approach of the exact pseudodata to $P_L(y)$ for $y < -1.5$ fm $^{-1}$ is extremely slow with increasing q . There is even the danger that at not too large q 's, the pseudodata seem to scale without having reached the asymptotic value $P_L(y)$. Though for certain q and y intervals scaling is violated the formal result is that the pseudodata for the potentials considered scale to the correct limit function $P_L(y)$ in the limit $q \rightarrow \infty$. According to our numerical experience that limit in q is not uniform in y . An interpretation of the pseudodata neglecting the final-state interaction is highly insufficient except for the immediate neighborhood of the quasielastic peak. The q dependence of the scaling function $(q/2m)S$ for fixed y 's (see Figs. 6 and 7) shows a rich structure varying with y , which results from the interplay of the bound-state wave function and the half-shell two-body T matrices. Precise experiments would provide interesting insight into these quantities.

With respect to the question of interference terms we found in our model that they can be neglected above $q \approx 5$ fm $^{-1}$, but are noticeable below. Hence, we expect a similar scaling behavior for ${}^3\text{He}$ and the deuteron above $q \approx 5$ fm $^{-1}$.

The representation of the structure function by a few low-order cumulants turned out to be unsuccessful. We showed analytically that $S(q, \omega) = O(\omega^{-5.5})$ for Yukawa interactions. This tells that higher-order cumulants do not exist.

One of the authors (W.G.) would like to thank R. Rosenfelder for very informative discussions on the subject.

¹G. B. West, Phys. Rep. C **18**, 263 (1975).

²R. Rosenfelder, Ann. Phys. **128**, 188 (1980).

³S. A. Gurvitz and A. S. Rinat, Phys. Rev. C **35**, 696 (1987).

⁴R. A. Malfliet and J. A. Tjon, Nucl. Phys. A **127**, 161 (1969).

⁵For more details of that work see, D. Hüber, Diploma thesis, Ruhr-Universität Bochum, 1989 (unpublished).

⁶A. S. Rinat and R. Rosenfelder, Phys. Lett. B **193**, 411 (1987).

⁷V. R. Pandharipande and R. Schiavilla, in Nucl. Phys. A **508**, 423c (1990).

⁸J. Holz and W. Glöckle, J. Comput. Phys. **76**, 131 (1988).

⁹J. G. Zabolitzky and W. Ey, Phys. Lett. **76B**, 527 (1978).

¹⁰C. Ciofi degli Atti, E. Pace, and G. Salmè, Phys. Rev. C **36**, 1208 (1987).

¹¹R. G. Arnold *et al.*, Phys. Rev. Lett. **61**, 806 (1988).